ACTA ASTRONOMICA
Vol. **57** (2007) pp. 173–199

A Study of Stellar Photometric Variability Within the Central 4 pc of the Galactic Center with Infrared Image Subtraction[1]

M. S. Peeples, K. Z. Stanek and D. L. DePoy

Department of Astronomy, Ohio State University, 140 W. 18$^{\rm th}$ Ave.,
Columbus, OH 43210, USA
e-mail(molly,kstanek,depoy)@astronomy.ohio-state.edu

Received March 29, 2007

ABSTRACT

We present a catalog of 110 variable stars within $\approx 1'$ of Sgr A* based on image subtraction of near-infrared (*H* and *K*) photometry. Our images were obtained over 133 nights from 2000 to 2002 in *H*-band and over 134 nights from 2001 to 2002 in *K*-band; the typical FWHM is $1\farcs4$. We match the catalog to other near-infrared, X-ray, and radio (*i.e.*, maser) data, and we discuss some of the more interesting objects. The catalog includes 14 sources with measurable periods, several known long-period variables and three new LPV candidates. We associate IRS 10* with OH, SiO, and H_2O masers and a bright X-ray point source; this analysis suggests IRS 10* is an AGB star with an accreting companion. Among the ≈ 90 newly discovered sources are a probable cataclysmic variable, a potential edge-on contact 84 day period eclipsing binary, and a possible 41 day period pulsating variable.

Key words: *Galaxy: center – Stars: variables: general*

1. Introduction

The Galactic center offers a unique opportunity for studying star formation and stellar populations near a supermassive black hole (SMBH), namely, Sgr A*. Active galactic nuclei and supernovae feedback have been evoked to explain many of the observed inhomogeneities in different galaxies (*e.g.*, Silk 1997, Efstathiou 2000, Scannapieco *et al.* 2005), but it is only in our own Galaxy that we are able to resolve individual stars within the circumnuclear ring surrounding the central SMBH (Jackson *et al.* 1993). Within the Milky Way, the cluster of stars at the Galactic center is also unique in that it is comprised of both old and young stars (see *e.g.*, Lacy *et al.* 1982, Paumard *et al.* 2006). It is believed that the young stellar population is the result of a burst of star formation at the Galactic center a few Myr ago (Krabbe *et al.* 1995), and that perhaps Sgr A* was more actively accreting

[1]Based on observations from the CTIO/Yale 1-m telescope with the ANDICAM imager.

mass than it is observed to be today. Furthermore, there is evidence that the stellar initial mass function near a SMBH is top heavy (Nayakshin and Sunyaev 2005), implying that the Galactic center is a viable location for finding highly massive stars. Photometric variability is one way of probing the mixed Galactic center stellar population on a large scale, as both evolved low mass and high mass stars are prone to photometric variations.

There have been several photometric variability studies of the Galactic center, some of which we summarize in Table 3. While some of these studies have covered a much longer baseline than ours does (*e.g.*, Ott *et al.* 1999, Rafelski *et al.* 2007), with more than 130 epochs in each band, our light curves have a much higher sampling. These data also represent the first major multi-wavelength photometric variability study of the Galactic center since Blum *et al.* (1996a).

We present here our catalog of 110 variable stars within ≈ 2 pc of Sgr A*, including 14 periodic sources. We outline our observations in Section 2. In Section 3 we discuss the reduction of data with image subtraction. We discuss our variable selection in Section 4, and we present the catalog of variables and their light curves along with a discussion of some of the more well-known and interesting objects in Section 5. We adopt a galactocentric distance of 7.6 kpc (Eisenhauer *et al.* 2005).

2. Observations

The observations from which IRS 16SW was studied by DePoy *et al.* (2004) and Peeples *et al.* (2007a) were of a field of view of $112'' \times 112''$ (4.12 pc projected) approximately centered on the Galactic center; we describe here the stellar photometric variability in these data. The observations of the Galactic center were made from 2000–2002 at the Cerro-Tololo Inter-American Observatory (CTIO)/Yale 1-m telescope using the facility optical/infrared imager (ANDICAM; see DePoy *et al.* 2003 for details). ANDICAM has a pixel scale of $0\overset{''}{.}22$/pix on a 1024×1024 array. Both *H*- and *K*-band (centered at 1.6μm and 2.2μm respectively) images were taken in the 2001 and 2002 observing seasons; *H*-band data were also obtained in 2000. The observing campaign consists of every usable night from UTC 2000 August 13 through UTC 2000 October 14, UTC 2001 May 20 through UTC 2001 November 3, and UTC 2002 June 9 through UTC 2002 September 25. Each night, a set of seven slightly offset images were obtained and then combined and trimmed (decreasing the field of view) to form a final nightly image. The *H*-band images consist of 30 s exposures, and it took about four minutes to obtain the group of seven images; the *K*-band images consist of 10 s exposures and it took about two minutes to obtain all components.

After image quality cuts were made, there are a total of 133 *H*-band images spanning 774 nights and 134 *K*-band images spanning 495 nights. The full-width half-maximum (FWHM) ranges from $0\overset{''}{.}93$ to $1\overset{''}{.}93$; in general, the *H*-band images are of somewhat higher quality (typical FWHM $\approx 1\overset{''}{.}3$) than the *K*-band (with typical FWHM $\approx 1\overset{\prime\prime}{.}45$). The final H- and K-band images are also offset relative to one another by $8.8''$; most of the detections of stars in only one of the two bands are due to this offset.

3. Data Analysis

Because the field is crowded, we reduced the data with the ISIS image subtraction package (Alard and Lupton 1998, Alard 2000) following the procedures outlined by Hartman *et al.* (2004). ISIS measures the change in flux for an object relative to a reference image, after correcting for the relative change in the point spread function (PSF). Our reference images (and thus "fiducial" magnitudes) for both bands are based on images from the 2001 observing season. The reference H-band image is presented in Fig. 1.

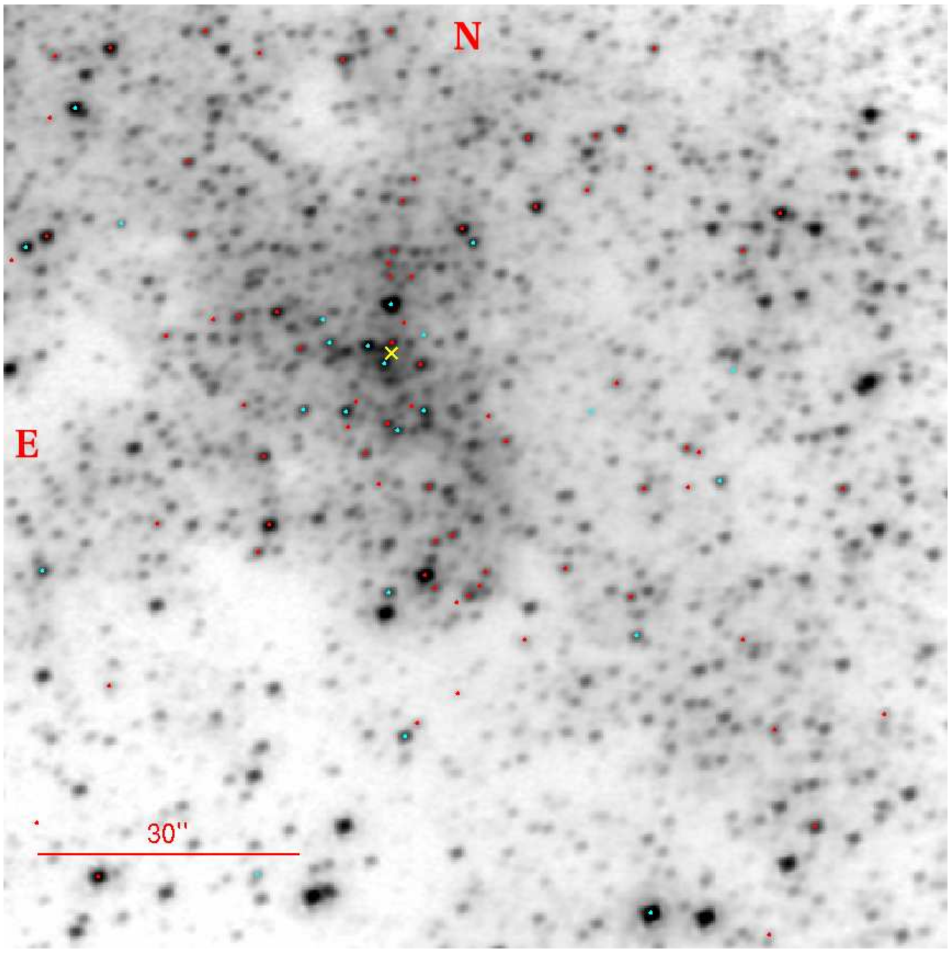

Fig. 1. The reference H-band image. The gray and black points mark variable sources listed in Tables 1 and 2; the gray points mark stars discussed in Section 5. The 'X' marks the location of Sgr A*. North is up and East is to the left.

Table 1

Catalog of variable stars

ID	$\Delta\alpha$ [arcsec]	$\Delta\delta$ [arcsec]	H [mag]	K [mag]	Common Names and Notes
PSD J174535.45-290007.6	−68.9	15.1	12.6		
PSD J174535.89-290113.5	−62.2	−50.8	14.2	10.9	
PSD J174535.98-290011.5	−60.9	11.3	12.1	9.7	
PSD J174536.18-290047.6	−57.9	−24.9	12.4	9.6	
PSD J174536.53-290125.9	−52.6	−56.8	11.9	9.5	
PSD J174536.63-290015.4	−51.2	7.3	10.7	8.8	
PSD J174536.85-290114.5	−47.8	−51.8	13.1	10.1	
PSD J174536.97-290138.0	−46.2	−75.3	15.0	10.2	
PSD J174536.97-290019.4	−46.1	3.3	12.5	10.0	
PSD J174537.10-290103.9	−44.1	−41.2	13.9	10.8	
PSD J174537.24-290045.7	−42.0	−23.0	12.6	9.9	V4910 Sgr
PSD J174537.42-290042.2	−39.3	−19.5	13.8	10.6	
PSD J174537.52-290046.2	−37.9	−23.4	14.5	10.6	
PSD J174537.52-290041.7	−37.8	−19.0	12.8	10.0	
PSD J174537.66-285955.2	−35.7	27.4	12.7		
PSD J174537.74-290009.2	−34.4	13.5	13.1	10.2	
PSD J174537.91-290045.9	−32.0	−23.2	12.7	10.0	
PSD J174537.98-290134.4	−30.9	−71.7	9.5	8.6	CXOGC J174537.9-290134
PSD J174537.98-290004.4	−30.9	18.3	12.0	9.2	
PSD J174538.02-290102.6	−30.3	−39.9	12.5	9.3	V4911 Sgr; blended
PSD J174538.05-290058.1	−29.7	−35.4	12.7	10.2	
PSD J174538.10-290033.5	−29.0	−10.9	13.3	10.3	
PSD J174538.19-290005.0	−27.7	17.7	12.5	9.7	
PSD J174538.29-290011.1	−26.2	11.6	13.4	9.9	
PSD J174538.61-290054.3	−21.4	−31.6	13.0	9.5	
PSD J174538.74-290012.7	−19.4	10.0	11.1	9.2	
PSD J174538.79-290004.6	−18.8	18.1	11.8	9.3	
PSD J174538.95-290139.6	−16.3	−77.0		9.4	
PSD J174538.99-290102.2	−15.7	−39.6	14.3	12.4	
PSD J174539.09-290039.3	−14.2	−16.6	12.7	9.8	blended
PSD J174539.23-290036.3	−12.1	−13.6	14.1	10.8	
PSD J174539.31-290016.3	−11.0	6.4	11.6	9.2	CXOGC J174539.3-290016
PSD J174539.31-290054.1	−11.0	−31.5	12.6	10.0	
PSD J174539.36-290055.6	−10.1	−33.0	13.0	10.5	
PSD J174539.39-290014.6	−9.7	8.0	10.9	8.4	blended
PSD J174539.45-290056.6	−8.8	−33.9	12.4	9.1	blended
PSD J174539.56-290057.3	−7.1	−34.7		12.5	
PSD J174539.58-290049.5	−6.9	−26.8	12.4	9.6	
PSD J174539.60-290107.6	−6.6	−44.9	15.3	11.8	*H* past threshold
PSD J174539.73-290050.2	−4.6	−27.5	12.5	9.9	

T a b l e 1

Continued

ID	Δα [arcsec]	Δδ [arcsec]	H [mag]	K [mag]	Common Names and Notes
PSD J174539.75-290055.5	−4.3	−32.8	12.5	9.6	IRS 22
PSD J174539.76-290026.4	−4.1	−3.7	14.1	10.6	IRS 34W
PSD J174539.77-290043.9	−4.0	−21.2	12.1	9.6	
PSD J174539.79-290008.5	−3.6	14.2	11.4	8.5	
PSD J174539.79-290029.9	−3.6	−7.2	13.2	10.6	IRS 13E
PSD J174539.83-290053.9	−3.1	−31.2	9.6	7.6	blended
PSD J174539.86-290024.7	−2.7	−2.0		10.5	
PSD J174539.86-290019.7	−2.6	3.0	12.8	10.0	
PSD J174539.90-290034.5	−2.1	−11.8	13.3	10.6	blended
PSD J174539.91-290011.0	−2.0	11.7	12.5	9.9	CXOGC J174539.9-290012
PSD J174539.93-290024.9	−1.6	−2.3	13.9	10.5	
PSD J174539.95-285951.1	−1.4	31.6	12.2		
PSD J174539.95-290110.8	−1.3	−48.2	14.2	10.2	
PSD J174539.99-290016.5	−0.7	6.2	12.1	9.8	IRS 15SW
PSD J174540.02-290037.2	−0.3	−14.5	11.8	9.4	IRS 14SW
PSD J174540.04-290018.0	0.0	4.7	12.3	10.3	IRS 15NE
PSD J174540.04-290022.7	0.0	0.0	9.0	—	IRS 7, saturated in K
PSD J174540.04-290027.0	0.0	−4.3	11.6	9.3	IRS 16NW
PSD J174540.04-290019.5	0.1	3.2	12.6		
PSD J174540.06-290112.1	0.4	−49.4	12.0	9.9	
PSD J174540.11-290036.4	1.0	−13.7	11.8	9.1	IRS 14NE
PSD J174540.21-290043.2	2.6	−20.5	14.1	10.7	
PSD J174540.21-290056.3	2.6	−33.6	15.6		
PSD J174540.31-285953.8	4.1	28.9	13.0		
PSD J174540.31-290039.5	4.1	−16.8	12.3	9.4	
PSD J174540.37-285954.0	5.0	28.7	11.7		blended
PSD J174540.38-290033.6	5.1	−10.9		11.4	
PSD J174540.45-290036.3	6.2	−13.6	13.8	11.1	CXOGC J174540.4-290036
PSD J174540.47-290034.6	6.4	−11.9	11.3	8.6	IRS 9, blended
PSD J174540.58-290026.7	8.2	−4.0	11.9	9.2	IRS 1NE
PSD J174540.64-290023.6	7.8	−1.4		10.2	IRS 10*, blended[a]
PSD J174540.83-290034.0	11.9	−11.4	12.2	9.1	IRS 28
PSD J174540.84-290027.0	12.0	−4.4	12.0	9.5	IRS 32
PSD J174541.04-290022.7	15.0	0.0	11.1	8.5	
PSD J174541.09-285952.6	15.8	30.1	13.2		
PSD J174541.17-290046.9	17.0	−24.2	10.7	7.9	IRS 19, blended
PSD J174541.20-290039.0	17.4	−16.3	11.6	9.1	
PSD J174541.27-290049.9	18.5	−27.2	12.8	9.6	
PSD J174541.35-290033.0	19.6	−10.4	13.2	10.2	

[a]This position is from Ott *et al.* (1999)

Table 1

Concluded

ID	Δα [arcsec]	Δδ [arcsec]	*H* [mag]	*K* [mag]	Common Names and Notes
PSD J174541.36-290022.7	19.8	−0.1	11.9	9.4	
PSD J174541.39-290126.6	20.3	−64.0	13.9	9.6	
PSD J174541.56-285949.6	22.9	33.1	12.4		
PSD J174541.59-290023.0	23.3	−0.4	13.7	10.8	
PSD J174541.75-290004.6	25.7	18.1	12.1	9.0	
PSD J174541.75-290013.0	25.7	9.7	12.3	9.3	
PSD J174542.01-290024.4	29.6	−1.8	13.2	10.0	
PSD J174542.13-290045.8	31.5	−23.1	13.5	10.3	
PSD J174542.39-285950.7	35.3	32.0	10.8		
PSD J174542.60-290103.9	38.5	−41.2	14.3	11.0	
PSD J174542.72-285957.4	40.2	25.3	10.5	7.7	V4928 Sgr, blended
PSD J174542.76-290125.5	40.9	−62.8	10.7	8.7	
PSD J174542.88-285951.3	42.6	31.4	12.7		
PSD J174542.92-285958.4	43.3	24.3	14.2	11.8	
PSD J174543.01-290011.9	44.6	10.7	10.8	8.5	
PSD J174543.19-290013.0	47.2	9.7	10.9	8.2	V4930 Sgr, blended
PSD J174543.29-290118.8	48.8	−56.2		11.9	
PSD J174543.31-290014.3	49.1	8.4	14.8	12.6	
PSD J174543.50-290005.3	52.0	17.4		9.0	

Non-periodic variable sources, sorted by RA. $\Delta\alpha$ and $\Delta\delta$ are with respect to IRS 7 at $(\alpha,\delta) = 17^{\rm h}45^{\rm m}40\overset{\rm s}{.}04, -29°00'22\overset{''}{.}7$, J2000.0 (Blum *et al.* 2003). In these coordinates, Sgr A* ($(\alpha,\delta) = 17^{\rm h}45^{\rm m}40\overset{\rm s}{.}04, -29°00'28\overset{''}{.}1$, J2000.0) is at $(\Delta\alpha,\Delta\delta) = (0\overset{''}{.}0, -5\overset{''}{.}4)$. The magnitudes listed are the fiducial magnitudes calculated from the ISIS reference image (see Section 3); these magnitudes are not mean magnitudes.

We identified the stars running DAOPHOT/ALLSTAR PROGRAM (Stetson 1987, Stetson 1992) on the astrometric reference image for each band. The final list consists of 1665 sources in *H*-band, with $H = 9.1$ mag to 17.0 mag, and 1785 sources in *K*-band, with $K = 7.7$ to 15.1 mag. We based the astrometric and photometric calibration on the 2MASS catalog (Strutskie *et al.* 2006). For the astrometry, we obtained an astrometric solution by matching the 2MASS *K*-band catalog to our *K*-band data. We similarly solved for the coordinate transformation between the *H*- and *K*-band data sets, which enabled us to find the coordinates of sources detected only in *H*-band. The astrometric solution is good to $\pm 0\overset{''}{.}24$ in RA and $\pm 0\overset{''}{.}21$ in dec (about ± 1 pixel in both coordinates). We calibrated our absolute photometry using this same set of stars matched to the 2MASS catalog; the photometric calibration error is ± 0.03 mag.

Table 2

Catalog of periodic variable stars

ID	$\Delta\alpha$ [arcsec]	$\Delta\delta$ [arcsec]	H [mag]	K [mag]	Period [days]	Notes
PSD J174535.60-290035.4	−66.6	−12.7	14.5	12.3	41.3 ± 0.5	CXOGC J174535.6-290034
PSD J174537.11-290033.1	−44.0	−10.4	10.0	12.8	188.4 ± 6.8	
PSD J174538.28-290006.8	−26.5	15.9	11.9	9.3	251.0 ± 8.4	
PSD J174538.35-290036.7	−25.5	−14.0	14.9	12.1	42.4 ± 0.8	
PSD J174538.97-290123.7	−16.1	−60.9	14.6	10.8	258.9 ± 8.3	
PSD J174538.98-290007.7	−16.0	15.0	13.0	9.9	325.3 ± 3.5	
PSD J174539.39-290039.5	−9.8	16.8	11.9	9.8	84.0 ± 1.3	
PSD J174539.79-290035.2	−3.8	−12.5	11.8	8.8	215.0 ± 2.4	IRS 12N, very blended
PSD J174540.12-290029.6	1.2	−6.8	10.8	8.3	19.4513 ± 0.0011	IRS 16SW
PSD J174540.13-290016.8	1.3	5.9	12.1	9.4	354.7 ± 4.2	IRS 15N, blended
PSD J174540.16-290055.7	1.7	−32.9	12.1	9.3	214.9 ± 2.6	CXOGC J174540.1-290055
PSD J174542.36-290011.2	34.8	11.6	13.4	10.6	221.6 ± 2.6	
PSD J174540.25-290027.2	3.2	−4.6	10.5	8.3	207.1 ± 6.1	IRS 16NE
PSD J174543.14-290050.2	46.5	−27.5	12.0	9.1	376.8 ± 4.1	blended

$\Delta\alpha$ and $\Delta\delta$ are with respect to IRS 7 at $(\alpha,\delta) = 17^{h}45^{m}40\overset{s}{.}04, -29^{\circ}00'22\overset{''}{.}7$, J2000.0. The magnitudes listed are the fiducial magnitudes calculated from the ISIS reference image (see Section 3); these magnitudes are not mean magnitudes. Except for IRS 16SW, the listed uncertainties on the periods roughly correspond to FWHM of the AoV peak (see Section 3). For IRS 16SW, the listed period and uncertainty are from Peeples *et al.* 2007a (see also Section 5.10).

We define the limiting magnitude for each band to be where the magnitude distribution peaks, as denoted by the vertical dashed lines in Fig. 2; this is approximately the magnitude at which the sky level starts to dominate the signal. The limiting *H*-band magnitude is 15.1 mag, and the limiting *K*-band magnitude is 12.6 mag; because these magnitude determinations are based on composite images (as opposed to individual images), the actual limiting magnitudes for individual observations of variable sources are significantly lower. The color–magnitude diagram is presented in Fig. 3.

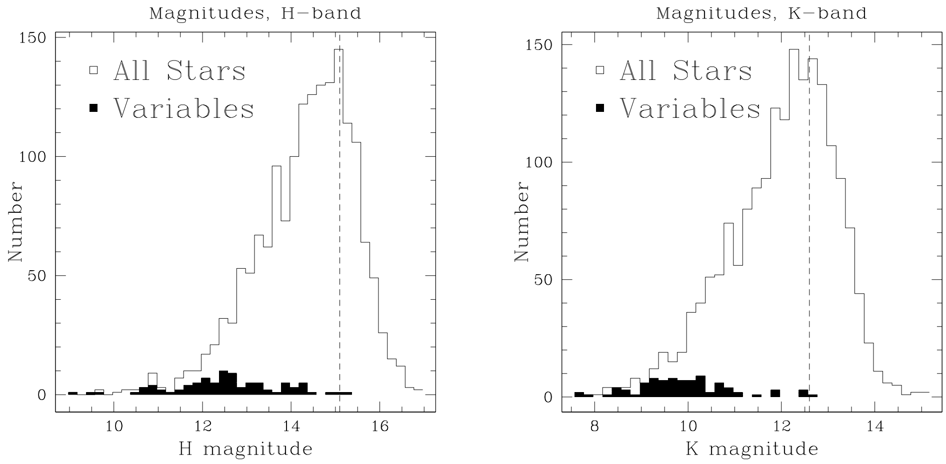

Fig. 2. Distribution of magnitudes in *H*-band (*left*) and *K*-band (*right*) for all detected sources. The vertical dashed lines are at the limiting magnitude for each band (see Section 3). The shaded histograms are the distribution of all variable sources; the variable sources fainter than the limiting magnitude are those sources which, while detected in both bands, are brighter than the limiting magnitude in one band, but below the limiting magnitude in the other band.

4. Variable Selection

The easiest to identify variable stars are those which vary about a mean magnitude more than typical stars of the same average magnitude. We therefore flagged potential variables independently in both *H*- and *K*-bands according to a root-mean-squared (rms) cut, as shown in Fig. 4. The cutoffs are given by

$$\log(\mathrm{rms,H}) \geq 0.377\,m_H - 6.044 \quad \text{and} \tag{1}$$

$$\log(\mathrm{rms,K}) \geq 0.370\,m_K - 5.192. \tag{2}$$

This led to $238/1665 = 14.3\%$ of *H*-band sources and $223/1785 = 12.5\%$ of *K*-band sources being flagged as potential variables. Each potential variable was visually inspected by two of us (M.S.P. and K.Z.S.), and flagged as "periodic" (if an AoV test yielded a believable period), "long term," "suspected," or not variable. We

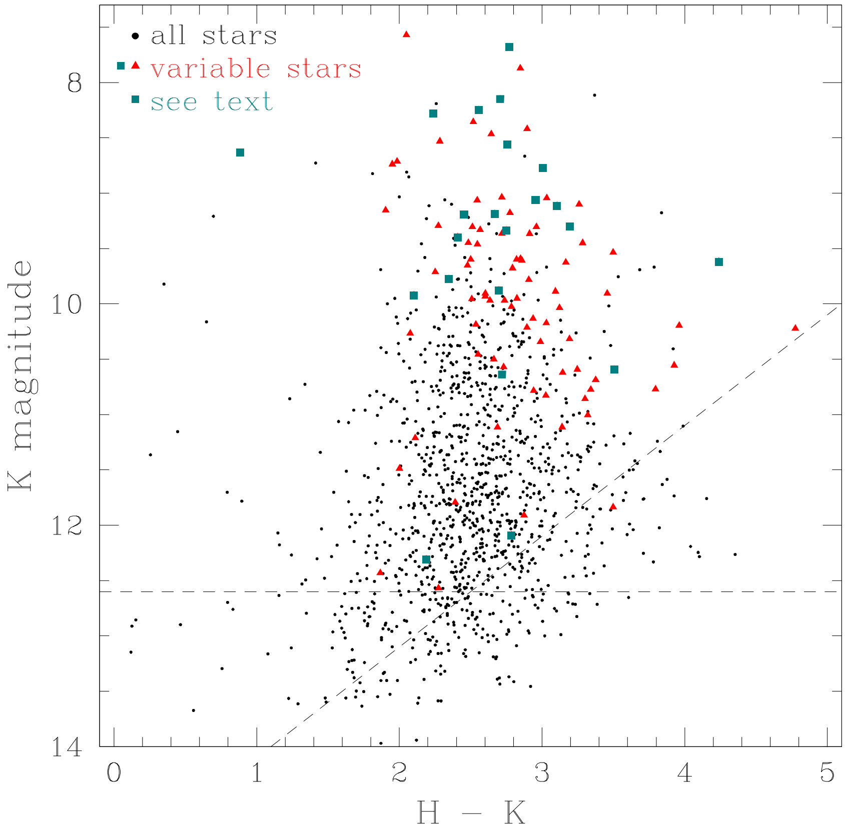

Fig. 3. Color-magnitude diagram. The red triangles and the cyan squares are variable sources; the cyan squares are the variable sources discussed in Section 5. Most of the spread in $H-K$ is due to differential reddening; the dashed lines correspond to the magnitude limits discussed in Section 3.

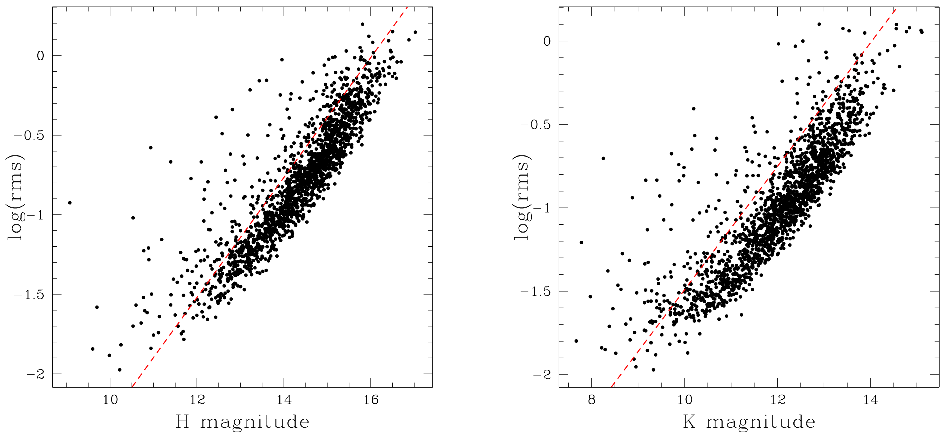

Fig. 4. Plots of log rms *vs.* magnitude for H (*left*) and K (*right*). Stars lying above the line were flagged as "potential variables."

also performed two period searches (AoV and LS; Schwarzenberg-Czerny 1996, Scargle 1982) on all of the sources. These searches revealed only two periodic sources not already flagged by the rms cut as well as three other clearly variable, low-amplitude non-periodic sources. The final sample includes 93 sources with both *H*- and *K*-band light curves, 14 of which are periodic, as well as 10 stars identified only in *H*-band and 7 stars identified only in *K*. The distribution of magnitudes for all of the variable sources are shown as the shaded regions of the histograms in Fig. 2.

Several of the sources flagged as variables were clearly blended, *i.e.*, nearby stars show similar light-curve shapes. As described in Section 4.6 of Hartman *et al.* (2004), the true variable is the one which displays the greatest amplitude of variability in flux. Thus, while in most cases we have not attempted to correct for blending, we are able to identify which sources are the true variables.

5. Catalog of Variables

The positions and magnitudes of our variable sources without clear period determinations are given in Table 1, and the light curves[2] are shown in Figs. 5–11. The periodic sources are summarized in Table 2 and Fig. 12.

In this Section, we discuss individual interesting variable sources. For previously identified sources, we compare our data to other studies. Table 3 summarizes some of the main near-infrared variability surveys of the Galactic center to date. At higher energies, Muno *et al.* 2004 used the *Chandra X-Ray Observatory* to study X-ray sources in the 0.5–8.0 keV band in the central 9′ of the Galaxy from September 1999 to June 2002. Of the more than 2000 point sources studied, 77 sources at the Galactic center displayed long-term variability. On the other end of the spectrum, several masers have been identified at the Galactic center. Specifically, Sjouwerman *et al.* (2002) studied twenty five 22 GHz H_2O masers within 2° and eighteen 43 GHz SiO masers within 15′ of Sgr A*; these masers are associated with OH stellar masers found by Lindqvist *et al.* (1992).

A summary of the sources discussed in this section is presented in Table 4; we first discuss previously identified sources, starting with the IRS sources (sorted numerically), followed by several sources also found by Glass *et al.* (2001) (sorted by their Samus and Durlevich 2004 variable catalog name). Finally, we discuss some of the more interesting new variables in our catalog; these subsections are sorted by RA, as in Tables 1 and 2.

5.1. IRS 1NE

IRS 1NE (PSD J174540.58-290026.7) passes the rms cut described in Section 4, but visually does not appear to vary over the timescales to which we are sensitive in this study. Ott *et al.* (1999) similarly found IRS 1NE to pass their χ^2

[2]Full light curves are available upon request from M. Peeples at molly@astronomy.ohio-state.edu

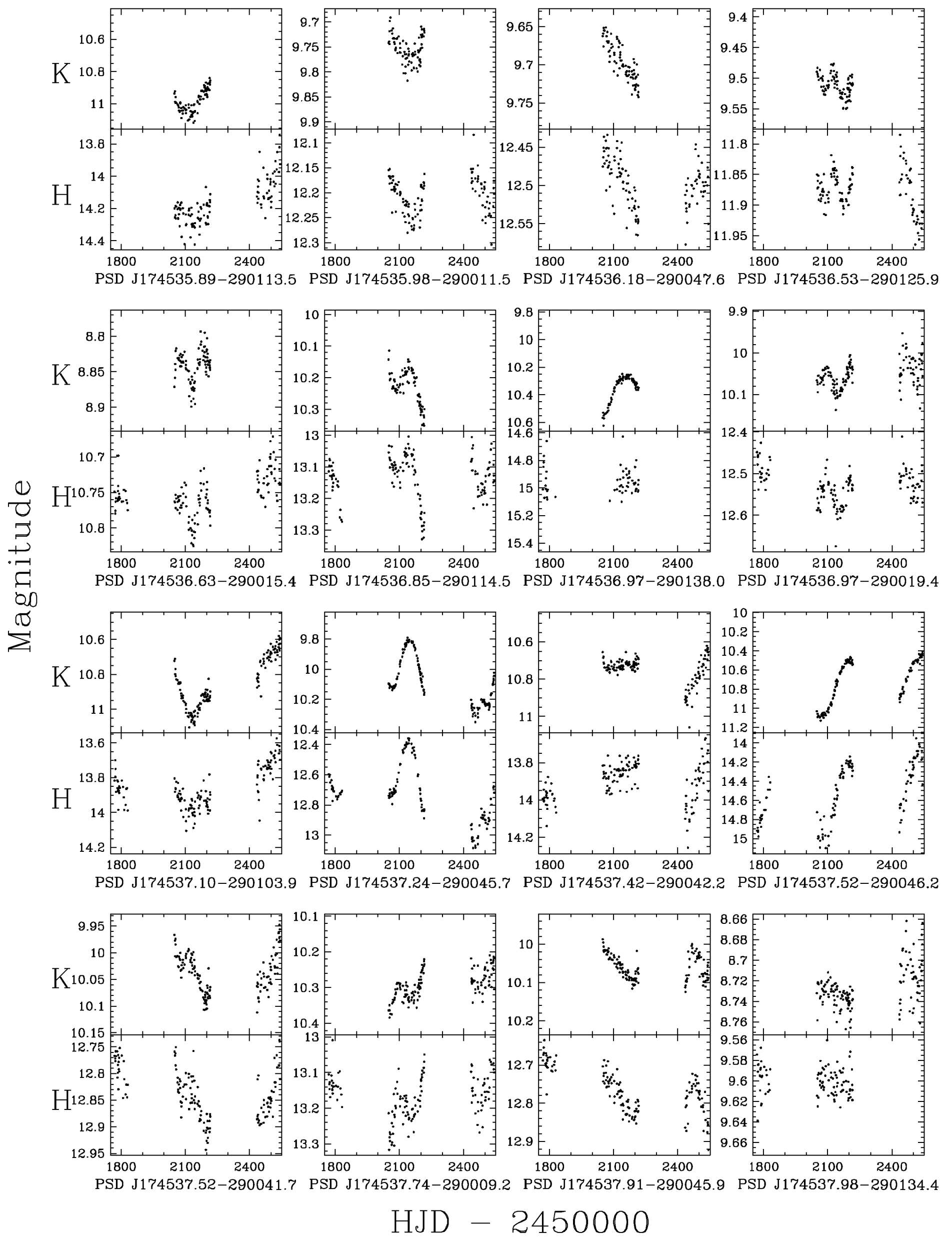

Fig. 5. Light curves of sources without clear period determinations detected in both *H* and *K*, sorted by RA as in Table 1. For each source, the extent of the *H*- and *K*-band ranges plotted is the same. Points lying below the magnitude limit (see Section 3) are not included.

variability cut, but this source did not pass their visual inspection test either. It is possible that IRS 1NE is in fact variable, but over shorter timescales to which either Ott *et al.*'s (1999) or our survey was sensitive, *i.e.*, $\lesssim 1$ day.

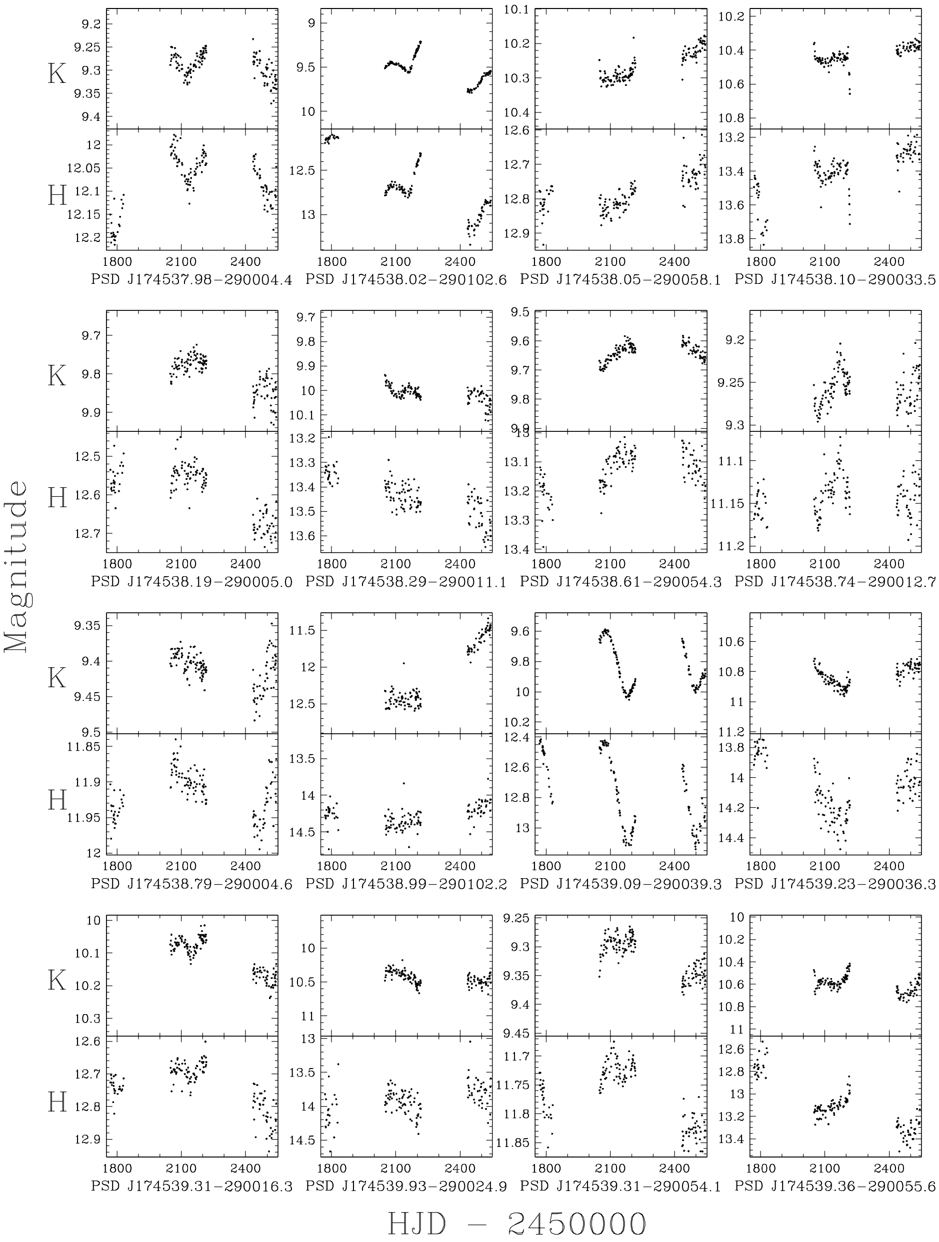

Fig. 6. Same as Fig. 5.

5.2. IRS 7

IRS 7 (PSD J174540.04-290022.7) is the brightest source in the field, and the only one to saturate in our *K*-band images. Ott *et al.* (1999) find this M2 supergiant long-period variable (LPV) to have a $\Delta K = 0.26$ mag. We find a $\Delta H = 0.33$ mag (from $H = 9.0$ mag to 9.33 mag).

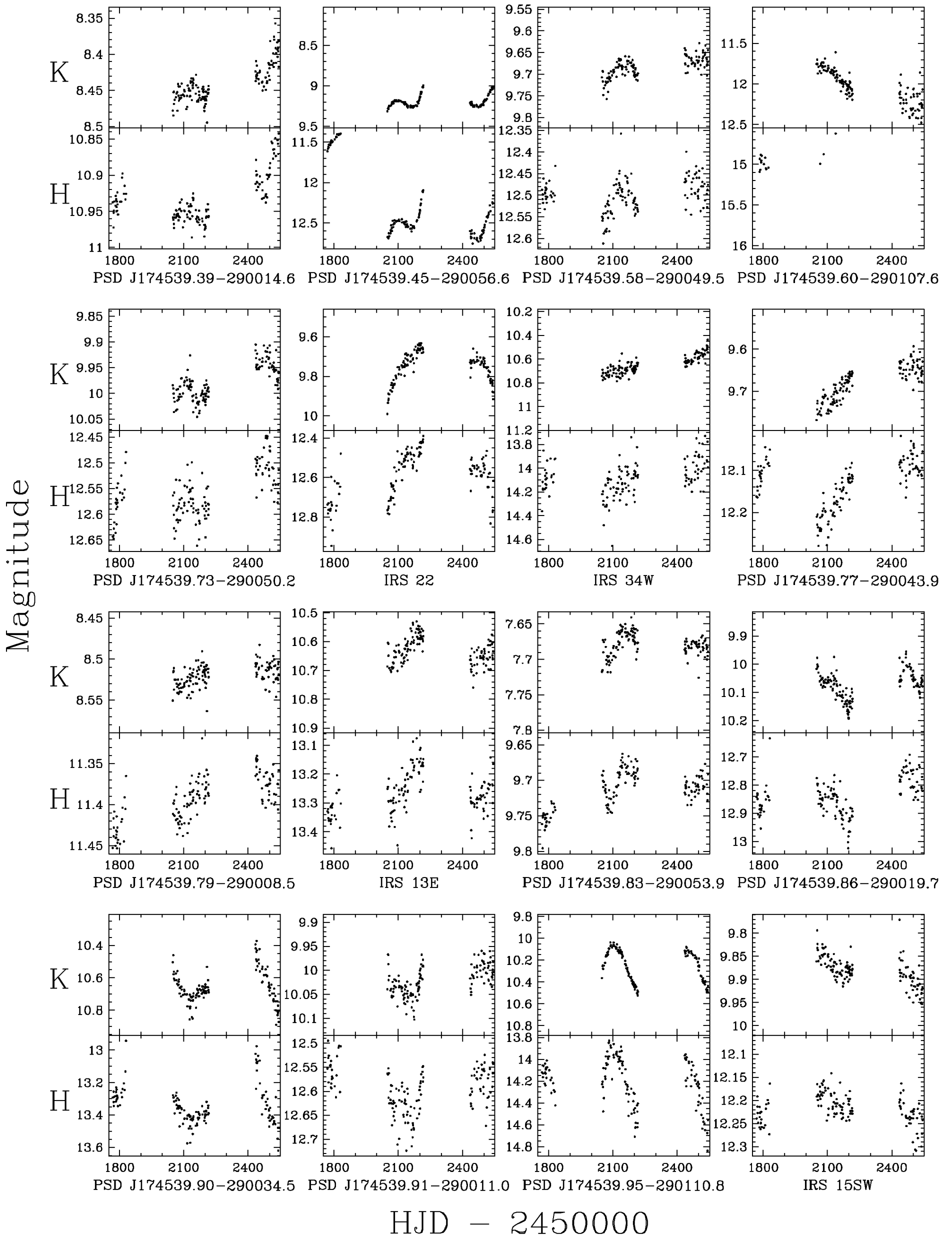

Fig. 7. Same as Fig. 5.

5.3. IRS 9

IRS 9 (PSD J174540.47-290034.6) is a large-amplitude variable, with $\Delta m_H =$ 0.92 mag and $\Delta m_K = 0.22$ mag (though most of the *H*-band large amplitude variability is seen in the year 2000, when no *K*-band data were taken). In our data, IRS 9 is blended with two stars detected in only *H*-band. Blum *et al.* (1096a) found

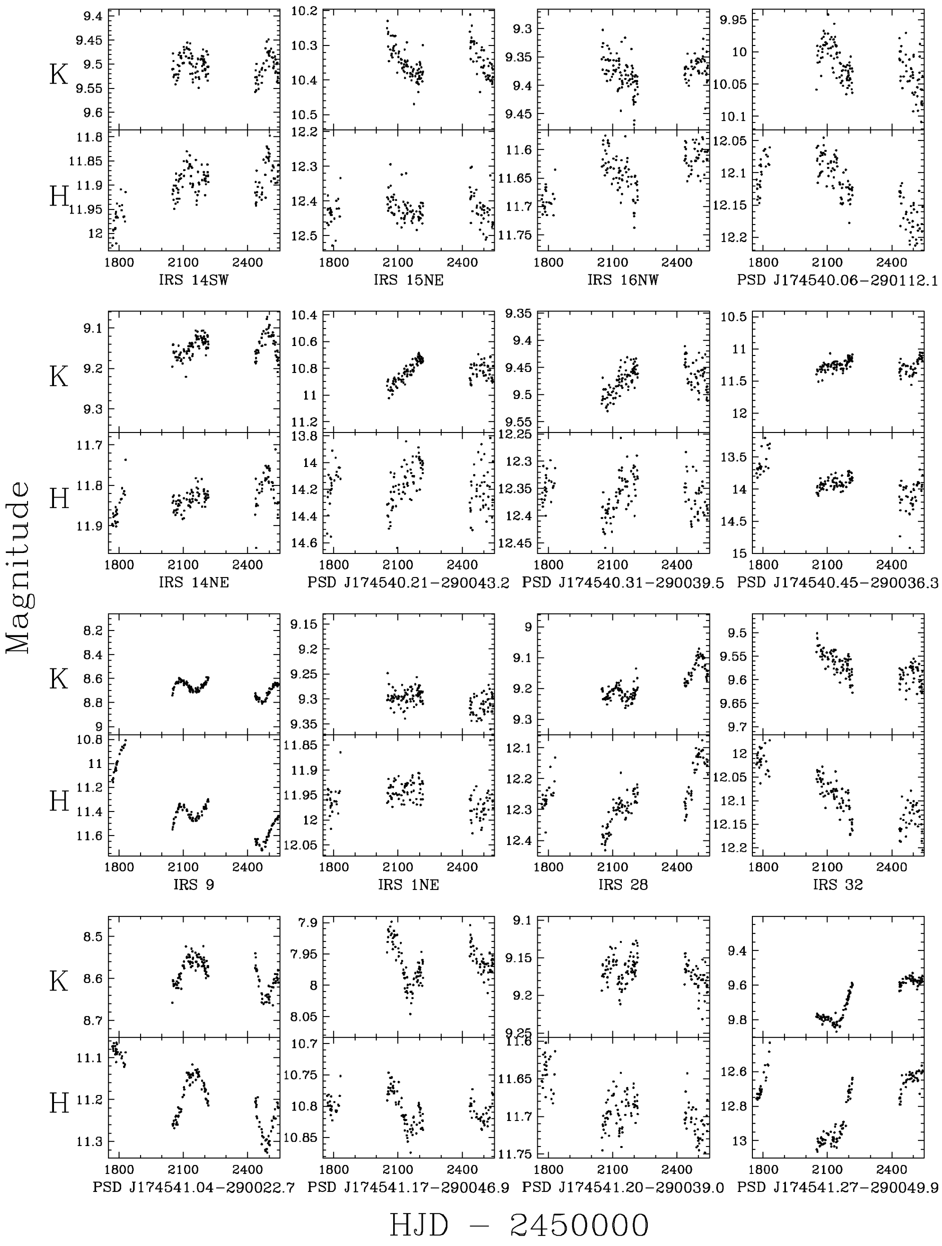

Fig. 8. Same as Fig. 5.

the $H-K$ color of this M7 LPV to change by ~ 0.2 mag from September 1989 to July 1993. Tamura *et al.* (1996) find IRS 9 to have brightened by ≈ 0.37 mag in *K*-band over about two years (from 1991 to 1993). Glass *et al.* (2001) find IRS 9 (their 3-2753, also known as V4920 Sgr) to have $\Delta m_K = 0.55$ mag over a period of 463 days; while our data do not rule out such a period, the light curve appears more consistent with that of a large-amplitude irregular or semi-regular variable.

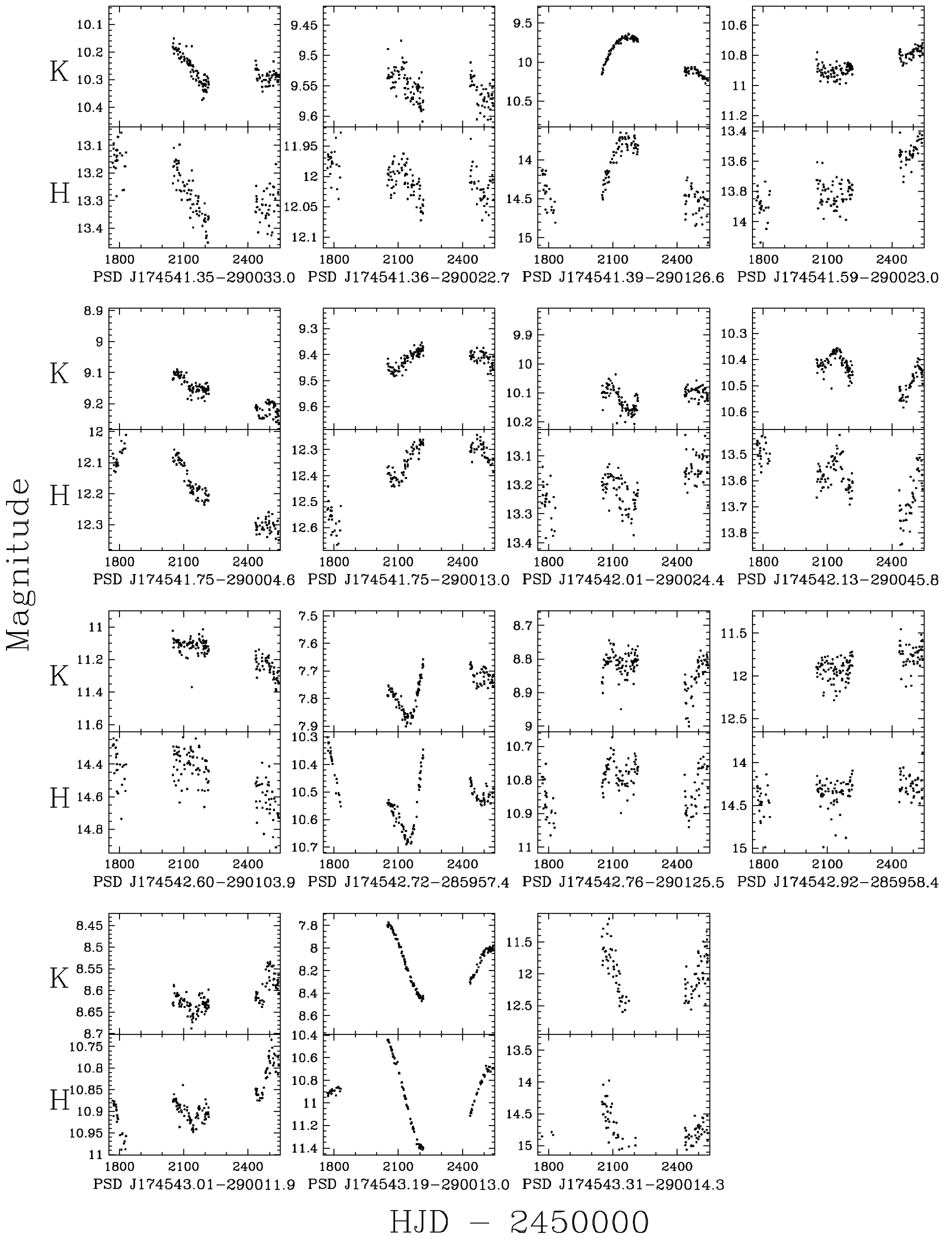

Fig. 9. Same as Fig. 5.

*5.4. IRS 10**

Tamura *et al.* (1996) found a variable source between IRS 10E and IRS 10W. Dubbed[3] IRS 10*, its brightness increased by at least one magnitude between 1991

[3]This source is referred to in the literature as IRS 10E*, IRS 10EL, and IRS 10EE; we will use here the original name IRS 10*.

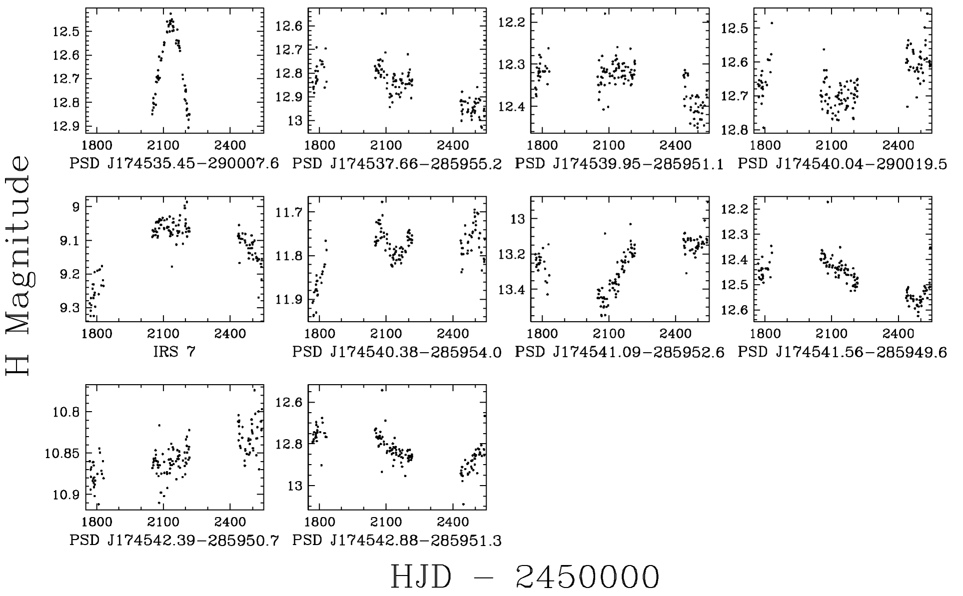

Fig. 10. Light curves of sources without clear period determinations detected only in *H*-band, sorted by RA as in Table 1. Points lying below the magnitude limit (see Section 3) are not included.

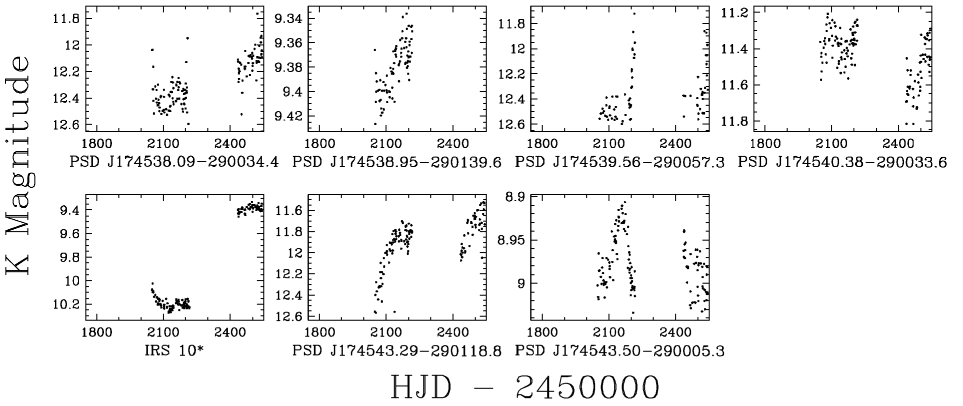

Fig. 11. Light curves of sources without clear period determinations detected only in *K*-band, sorted by RA as in Table 1. Points lying below the magnitude limit (see Section 3) are not included.

and 1992. Ott *et al.* (1999) found similar long-period brightness variations on the order of 1.4 mag. Like Tamura *et al.* (1996), we do not separately resolve IRS 10E, 10W, and 10*. In the subtracted images from ISIS, there appears to be only one point-source of variability in the IRS 10 region (*i.e.*, IRS 10E and 10W are presumably non-varying). We associate this variability seen in the IRS 10 complex with IRS 10*, even though DAOPHOT detects two sources in *H*-band (apparently the brighter nearby IRS 10E and 10W) and only one source in *K*-band. Because of this, the position we state for IRS 10* (PSD J174540.64-290023.6) in Table 1

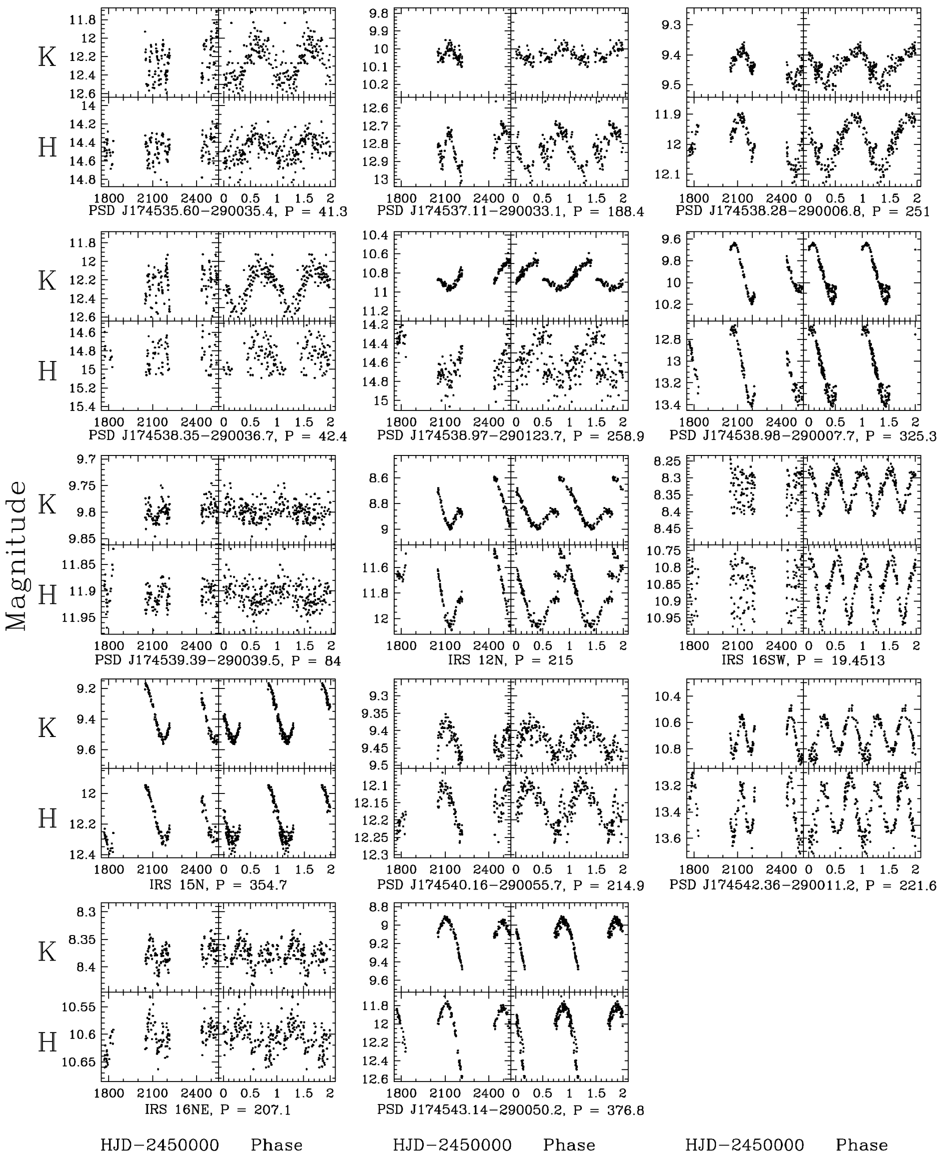

Fig. 12. Periodic sources. For each source, the extent of the *H*- and *K*-band ranges plotted is the same; the unphased light curves are shown in the *left panels* and the phased light curves are shown in the *right panels*. Points lying below the magnitude limit (see Section 3) are not included. All given periods *P* are in days.

is from Ott *et al.* (1999); the stated *K*-magnitude (10.2) is probably largely due to IRS 10E. We find the *K*-magnitude of IRS 10* to be relatively constant in both the 2001 and 2002 observing seasons, with the 2002 value being ≈ 0.8 mag brighter. Furthermore, IRS 10* was much redder in 2002 than it was in 2001.

Both Tamura *et al.* (1996) and Ott *et al.* (1999) associated IRS 10* with the OH maser OH 359.939-0.052 (Lindqvist *et al.* 1992), but Blum *et al.* (1996a,b)

Table 3

Near-infrared photometric surveys of the Galactic center

Survey	Field of view	Time sampling	Wavelength	Notes and Variable Sources
Tamura *et al.* 1996	$24'' \times 24''$	1991, 1992, 1993; 3 epochs	K	IRS 9, 10*, 12N, 14SW, 28
Blum *et al.* 1996a	central $\approx 2'$	May 1993 – April 1995; 5–8 epochs	J, H, K, L	IRS 7, 9, 12N
Ott *et al.* 1999	$20'' \times 20''$	August 1992 – May 1998; ≈ 40 epochs	K	IRS 7, 9, 10*, 12N, 16SW and potentially IRS 1NE, 6, 14SW
Glass *et al.* 2001	$24' \times 24'$	1994–1997; ≈ 30 epochs	K	only large-amplitude, periodic variability
Rafelski *et al.* 2007	$5'' \times 5''$	1995–2005; 50 epochs	K	IRS 16SW, 16NW, 16CC, 29N, and 12 S stars

For reference, $1''$ at 7.6 kpc (Eisenhauer *et al.* 2005, galactocentric distance) corresponds to 0.0368 pc projected; $1'$ corresponds to 2.211 pc projected.

associated it with the Lindqvist *et al.* (1992) maser OH 359.946-0.047[4]. Menten *et al.* (1997) found a SiO maser and Lindqvist *et al.* (1990) found a H_2O maser coincident with OH 359.946-0.047; Deguchi *et al.* (2002) and Sjouwerman *et al.* (2002) further found the SiO maser and the H_2O maser to be variable, respectively. Muno *et al.* (2004) additionally identify an X-ray source, CXOGC J174540.7-290024, within $0.''8$ of IRS 10* with an (unobscured) X-ray luminosity $L_X \approx 1.1 \times 10^{32}$ erg/s. Typically OH/IR stars are asymptotic giant branch (AGB) stars; these pulsating stars are experiencing mass loss, which accounts for both the NIR variability and the presence of masers. Genzel *et al.* (1996) spectroscopically confirm that IRS 10* (their IRS 10EE) is a late-type (*i.e.*, consistent with being an AGB) star.

While it is possible that the X-ray flux is due to some other nearby source (or collection of sources), under the assumption that all three masers and the X-ray source are associated with IRS 10* (and not IRS 10E or 10W), this might be the largest X-ray luminosity associated with an AGB star to date (Karovska *et al.* 2005). It has been proposed that AGB stars should be bright X-ray sources

[4] Though they are only two lines apart in Lindqvist *et al.*'s (1992) Table 2, OH 359.939-0.052 is roughly $35''$ further from the IRS 10 complex than OH 359.946-0.047.

Table 4

Summary of sources discussed in Section 5

ID	Fig.	Period	Classification	Alternate Name
IRS 1NE	8			PSD J174540.58-290026.7
IRS 7	10		LPV	PSD J174540.04-290022.7
IRS 9	8		LPV	PSD J174540.47-290034.6
IRS 10*	11		OH/IR, X-ray source	PSD J174540.64-290023.6
IRS 12N	12	215.0 ± 2.4	LPV	PSD J174539.79-290035.2
IRS 14SW	8			PSD J174540.02-290037.2
IRS 14NE	8		AGB	PSD J174540.11-290036.4
IRS 15SW	7		WR	PSD J174539.99-290016.5
IRS 16NE	12	207.1 ± 6.1	LBV?	PSD J174540.25-290027.2
IRS 16SW	12	19.451 ± 0.001	binary	PSD J174540.12-290029.6
IRS 28	8			PSD J174540.83-290034.0
IRS 34W	7		LBV?	PSD J174539.76-290026.4
V4910 Sgr	5			PSD J174537.24-290045.7
V4911 Sgr	6		SiO maser?	PSD J174538.02-290102.6
V4928 Sgr	9		OH/IR	PSD J174542.72-285957.4
V4930 Sgr	9		Mira	PSD J174543.19-290013.0
PSD J174535.60-290035.4	12	41.3 ± 0.5		
PSD J174538.34-290036.7	12	42.4 ± 0.8	binary??	
PSD J174538.98-290007.7	12	325.3 ± 3.5	LPV?	
PSD J174537.98-290134.4	5		X-ray source	
PSD J174539.31-290016.3	6		X-ray source	
PSD J174540.16-290055.7	12	214.9 ± 2.6	variable X-ray	
PSD J174541.39-290126.6	9		OH/IR	
PSD J174542.36-290011.2	12	221.6 ± 2.6		
PSD J174543.14-290050.2	12	376.8 ± 4.1		

Sources are sorted in the order they are discussed in Section 5; all given periods are in days.

($L_X \approx 10^{31}-10^{35}$ erg/s) due to strong magnetic fields, but various X-ray studies have not confirmed this prediction (*e.g.*, Soker and Zoabi 2002, Kastner and Soker 2004a,b); typical X-ray luminosities for, *e.g.*, Mira, are $\approx 10^{29}$ erg/s (Kastner and Soker 2004b). Soker and Zoabi (2002) suggest that AGB stars are radiating in the X-ray as proposed, but this radiation is not observed due to the high column density of the ejected material surrounding the star (see also Blackman *et al.* 2001). Furthermore, all AGB stars with detected X-ray radiation are in binary systems (*e.g.*, Mira A and B, Karovska *et al.* 2005); if this trend is in fact a prerequisite for a high AGB X-ray luminosity, then IRS 10* should have a companion. Because SiO, H_2O, and OH masers are believed to be due to different regions of the circumstellar envelope (SiO masers are relatively close to the star, H_2O masers are further out, and OH masers are even further away from the star; Reid and Moran 1981), the presence of all three masers implies that IRS 10* is enshrouded by a substantial circumstellar envelope. Yet as this material does not absorb the X-ray radiation, the X-ray flux is more likely to be due to accretion onto a companion star than the AGB star itself.

5.5. *IRS 12N*

Tamura *et al.* (1996), Blum *et al.* (1996a), Ott *et al.* (1999), and Glass *et al.* (2001) found IRS 12N (PSD J174539.79-290035.2, spectral type M7III) to be variable. Tamura *et al.* (1996) observed an increase of $\Delta m_K \approx 0.47$ mag over 2 years, and Ott *et al.* (1999) found similar variations. Glass *et al.* (2001) found IRS 12N (their 3-2753) to be a periodic variable of similar magnitude ($K = 8.74$) and amplitude ($\Delta m_K = 0.55$ mag) with a period $P = 463$ days. We cannot de-blend IRS 12N and IRS 12C; five variable sources are detected within $\approx 1\farcs5$ of IRS 12N with similar features to one another. We find this source to potentially be periodic, with $P = 215$ days or 429 days and a $\Delta K \gtrsim 0.4$ mag and a $\Delta H \gtrsim 0.65$ mag; no variations are observed on shorter timescales. These data are in agreement with the classification of IRS 12N as an LPV (Blum *et al.* (1996b).

5.6. *IRS 14SW*

IRS 14SW (PSD J174540.02-290037.2) is seen to have variability with amplitude ≈ 0.1 mag in both *H*- and *K*-bands in the 2001 and 2002 observing seasons. Additionally, the *H*-band light-curve is ≈ 0.1 mag lower in the 2000 observing season than in 2001–2002. Tamura *et al.* (1996) state that IRS 14SW is a “probable” variable; Ott *et al.* (1999) find that IRS 14SW passes their χ^2 cut, but they do not comment on its variability. It is clear from our data that IRS 14SW is, in fact, a variable source.

5.7. *IRS 14NE*

IRS 14NE (PSD J174540.11-290036.4) is a known AGB star (spectral type M7III; Blum *et al.* 1996b). Ott *et al.* (1999) find IRS 14NE to have $m_K = 9.45$ mag and amplitude $\Delta K = 0.15$ mag, though they do not flag it as a potential variable. This is consistent with our findings of $\Delta K \approx 0.14$ mag and $\Delta H \approx 0.16$ mag; we find its variability to have clear structure.

5.8. *IRS 15SW*

IRS 15SW (PSD J174539.99-290016.5) is a known Wolf-Rayet (WR) star (also known as WR 101i; van der Hucht 2001) with spectral type WN8/WC9 (Najarro *et al.* 1997, Paumard *et al.* 2006). We detect small-amplitude variations in IRS 15SW, with $\Delta m_K \approx \Delta m_H \approx 0.15$ mag.

5.9. *IRS 16NE*

Like many of the stars in the IRS 16 cluster, IRS 16NE (PSD J174540.25-290027.2) is a potential luminous blue variable (LBV) star (Clark *et al.* 2005) with spectral type Ofpe/WN9 (Paumard *et al.* 2006). We observe IRS 16NE to have an amplitude of only ≈ 0.11 mag in both *H* and *K*; furthermore, we do not observe the $H - K$ color to change substantially or systematically. On the other hand, the light curve is potentially consistent with a period of 207 days.

5.10. IRS 16SW

IRS 16SW (PSD J174540.12-290029.6) was originally proposed to be a massive eclipsing binary by Ott *et al.* (1999). Using the same data presented here, DePoy *et al.* (2004) proposed that IRS 16SW is instead a new kind of massive pulsating star, but a recent re-reduction of the data by Peeples *et al.* (2007a) revealed a sign error in the DePoy (2004) analysis. Martins *et al.* (2006) presented a radial velocity curve of IRS 16SW; while it appears to be a single-line binary, both their analysis and that of Peeples *et al.* (2007a) found the data to be consistent with a contact binary of twin 50 $M_\odot$ stars. While Rafelski *et al.* (2007) also support the idea that IRS 16SW is an eclipsing binary, their light curve shows an asymmetry in the rise- and fall-times – the rise-time appears to be ≈ 1.6 times that of the fall-time – which they propose is due to tidal deformations causing asynchronous rotational and orbital periods of the two stars. As discussed by Peeples *et al.* (2007a), our data do not show such a strong asymmetry; such an asymmetry is not seen by Martins *et al.* (2006) either.

5.11. IRS 28

IRS 28 (PSD J174540.83-290034.0) is another source described as a "probable" variable by Tamura *et al.* (1996). Blum *et al.* (1996b) classify IRS 28 as an LPV, and Glass *et al.* (2001) find IRS 28 (their 3-72, also known as V4923 Sgr) to be a periodic source with an amplitude of $\Delta m_K = 0.4$ mag and a period of $P = 195$ days. We find this source to not be clearly periodic (and a period of ≈ 200 days is ruled out). We find $\Delta m_K \approx 0.2$ mag and $\Delta m_H \approx 0.32$ mag; in the two observing seasons with both *H*- and *K*-band data, the two light-curves have similar structures, but the *H*-band light-curve clearly has a larger amplitude.

5.12. IRS 34W

Trippe *et al.* (2006) find IRS 34W (PSD J174539.76-290026.4) to be an irregular variable Ofpe/WN9 star, suggesting that it is a transitional object between the O supergiant and LBV phases of its evolution. We find an $H-K$ color of 3.5 mag, which is consistent with what Trippe *et al.* (2006) found for a similar epoch.

5.13. V4910 Sgr and V4911 Sgr

Glass *et al.* (2001) found V4910 Sgr (their 3-270, our PSD J174537.24-290045.7) to have a $K = 10.27$ mag and vary with amplitude 0.8 mag over a period of 601 days. We find V4910 Sgr to have $H = 12.6$ mag and $K = 9.9$ mag, with amplitudes $\Delta m_H = 0.73$ mag and $\Delta m_K = 0.56$ mag. While a period of ≈ 600 days is not ruled our by our data, this source appears to be an irregular or semi-regular large-amplitude variable with no convincing signs of periodicity.

Similarly, Glass *et al.* (2001) found V4911 Sgr (their 3-88, our PSD J174538.02-2901002.6) to have a $K = 9.58$ mag with amplitude 0.5 mag over a period of 528 days. We find V4911 Sgr to have $H = 12.5$ mag and $K = 9.3$ mag, with amplitudes

$\Delta m_H \approx 1.15$ mag and $\Delta m_K = 0.58$ mag (much of the variation seen in *H*-band is from the 2000 observing season, when no *K*-band data were taken). While a period of ≈ 528 days is not ruled out by our data, this source appears to be an irregular or semi-regular large-amplitude variable with no convincing signs of periodicity. Deguchi *et al.* (2002) associate V4911 Sgr with the SiO maser SiO 359.930-0.045, though the projected separation is $\approx 7''$.

5.14. V4928 Sgr

PSD J174542.72-285957.4 is one of the brightest stars in our sample. Also known as V4928 Sgr, this source is associated with OH, SiO, and H_2O masers, OH 359.956-0.050[5] at $\alpha = 17^h45^m42\overset{s}{.}763$, $\delta = -28°59'57\overset{''}{.}20$ (Deguchi *et al.* 2002, Sjouwerman *et al.* 2002). Glass *et al.* (2001) find V4928 Sgr (their 3–5) to have an m_K of 7.89 mag, with amplitude $\Delta m_K = 0.65$ mag and period $P =$ 607 days. We find amplitudes of $\Delta m_H \approx 0.4$ mag and $\Delta m_K \approx 0.25$ mag, but it is clear that the "true" amplitude is greater than this, as at the end of the 2001 observing season the light curve shows no signs of flattening. Though a period of ≈ 600 days does not appear consistent with our data, we cannot rule out that V4928 Sgr is indeed periodic. The observed large-amplitude variability in the presence of masers flags this source as an LPV candidate.

It is possible that V4928 Sgr is, in fact, the LPV IRS 24 (Blum *et al.* 1996a,b). The projected distance between IRS 24 (at $\alpha = 17^h45^m41\overset{s}{.}8$, $\delta = -28°59'59\overset{''}{.}51$ J2000.0) and V4928 Sgr is $13\overset{''}{.}6$; however, when Levine *et al.* (1995) first discovered an H_2O maser at $\alpha = 17^h45^m42\overset{s}{.}7$, $\delta = -28°59'57\overset{''}{.}2$ J2000.0, they associated it with the bright near-infrared IRS 24.

5.15. V4930 Sgr

V4930 Sgr (PSD J174543.19-290013.0) is a known Mira (LPV) variable (Samus and Durlevich 2004). We observe V4930 Sgr, which is one of the brightest variable stars in our sample, to smoothly vary with an amplitude of ≈ 1 mag in *H* and ≈ 0.7 mag in *K*. Glass *et al.* (2001) likewise find V4930 Sgr (their 3–16) to have an amplitude of $\Delta m_K = 1.0$ mag over a period of 554 days. While our *H*-band data do not rule out a period of ≈ 550 days, the light curve does not appear to be clearly periodic.

5.16. PSD J174535.60-290035.4 and PSD J174538.34-290036.7

PSD J174535.60-290035.4 and PSD J174538.34-290036.7 are two of the most enigmatic variables in our sample. For simplicity, in this Section alone, we will refer to PSD J174535.60-290035.4 as PSD 35.6-35.4 and PSD J174538.34-290036.7 as PSD 38.3-36.7. Both of these variables are clearly periodic. PSD 35.6-35.4 has a period $P = 41.3 \pm 0.5$ days with amplitude $\Delta m_K \approx 0.77$ mag and $\Delta m_H \approx 0.63$ mag; PSD 38.3-36.7 has a period $P = 42.4 \pm 0.8$ days with amplitudes $\Delta m_K \approx 0.66$ mag

[5] Ott *et al.* (1999) associate this maser with IRS 10*, but they are separated by $\approx 35''$.

and $\Delta m_H > 0.57$ mag (PSD 38.3-36.7 is quite faint in H-band). Because these periods, magnitudes, and variability amplitudes are so similar, we will discuss these two sources together.

One obvious intriguing possibility is that these stars are Cepheids. Both of these sources have $\langle m_K \rangle \approx 12.3$ mag; assuming these are Cepheids and taking $P = 42$ days, we can calculate the absolute K-band magnitude using the Cepheid period-luminosity relation from Benedict *et al.* (2007):

$$\langle M_K \rangle = -3.32[\log(P) - 1.0] - 5.71 = -7.78. \tag{3}$$

If we now assume that these stars are at the Galactic center, with $d_{\rm GC} = 7600$ pc, we can take this absolute magnitude and calculate the K-band extinction,

$$A_K = \langle m_K \rangle - \langle M_K \rangle - 5 \log d_{\rm GC,pc} + 5 = 5.68. \tag{4}$$

This A_K, which corresponds to an $A_V = A_K/0.112 = 50.7$ mag (Schlegel *et al.* 1998), is rather large, even for the Galactic center. Scoville *et al.* (2003) give A_V near PSD 38.3-36.7 to be ≈ 25 (derived from Paα to H92α radio recombination line-emission ratios) to ≈ 34 (derived from Paα to 6 cm radio continuum emission ratios); A_V is unmeasured near PSD 35.6-35.4. Another way of expressing this discrepancy is to say that if we use the Scoville *et al.*'s (2003) average A_K for the field, $A_K = 3.48$ mag, then Eq. (4) yields an $\langle M_K \rangle$ that is ≈ 2 mag fainter than is predicted by Eq. (3).

It is possible, of course, that the intervening dust is patchy on scales smaller than Scoville *et al.* (2003) could resolve, and that one or both of these stars happen to be behind a dense clump of obscuring material. Under the assumption that these stars are Cepheids, we can constrain the actual A_K for each source from the observed $H-K$ colors; Cepheids have an unreddened $\langle M_H - M_K \rangle \approx 0.0$ mag (Laney and Stobie 1994). Taking $A_H/A_V = 0.176$ and $A_K/A_V = 0.112$ from Schlegel *et al.* (1998), we find

$$A_K = \frac{E(H-K)}{0.176 - 0.122} \times 0.112 = 1.75E(H-K). \tag{5}$$

For $M_H - M_K = 0.0$, the observed $H-K$ color of 2.2 for PSD 35.6-35.4 yields $A_K = 3.85$ mag and the observed $H-K$ color of 2.6 for PSD 38.3-36.7 yields $A_K = 4.55$ mag. These extinction values are substantially less than the $A_K = 5.68$ mag calculated above; if either of these stars is in fact a Cepheid, some combination of a different reddening law or a different period-luminosity relation than used here would have to come into play.

If neither PSD 35.6-35.4 nor PSD 38.3-36.7 is a Cepheid, then the possible nature of the variability seen in these stars is unclear. The shape of the light curve of PSD 35.6-35.4 remains reminiscent of a pulsating variable; a steep brightening is followed by a longer fall-time. The light curve of PSD 38.3-36.7, however, is much more symmetric; it is possible that it is an eclipsing binary, perhaps similar to those found by Soszyński *et al.* (2004) in the Large Magellanic Cloud. If this is the case, then like IRS 16SW (see Section 5.10) it is close to the contact configuration (because the light curve does not flatten out of eclipse), composed of near-equal surface brightness stars (because the depths of the eclipses are the same), and we are viewing it almost edge-on (because the depths of the eclipses are close to 0.75 mag). These conditions are suspicious given that, if PSD 38.3-36.7 is a binary, then its period is 84.8 days. For comparison, IRS 16SW has a period of 19.45 days and is comprised of two $50M_\odot$ stars with a separation of $\approx 150R_\odot \approx 0.7$ a.u. (Martins *et al.* 2006, Peeples *et al.* 2007a). Spectroscopic monitoring is the only way to determine the nature of the variability of PSD 35.6-35.4 and to break the mass-radius degeneracy if PSD 38.3-36.7 is an eclipsing binary.

5.17. PSD J174538.98-290007.7

We observe PSD J174538.98-290007.7 to have a period of ≈ 325 days with an amplitude of 0.75 mag in *H*-band and 0.52 mag in *K*-band. Based on this large period and these large amplitudes of variation, we propose that PSD J174538.98-290007.7 is an LPV.

5.18. PSD J174537.98-290134.4 and PSD J174539.31-290016.3

We associate PSD J174537.98-290134.4 and PSD J174539.31-290016.3 with CXOGC J174537.9-290134 and CXOGC J174539.3-290016 respectively (Muno *et al.* 2004). PSD J174537.98-290134.4 has marginal variability, but it is a bright source ($H = 9.5$ mag and $K = 8.6$ mag). Muno *et al.* (2004) detected neither short-term nor long-term variability for either X-ray source.

5.19. PSD J174540.16-290055.7

PSD J174540.16-290055.7 is, within uncertainties, coincident with the long-term X-ray variable CXOGC J174540.1-290055 ($L_X \approx 10^{35}$ erg/s, Muno *et al.* 2004). We find this source to potentially be periodic, with a period of ≈ 215 days and an amplitude of $\Delta m_H = 0.2$ mag and $\Delta m_K = 0.15$ mag. Muno *et al.* (2004) observed the X-ray flux, on the other hand, to vary by a factor of five over the course of 17 days. These data are consistent with PSD J174540.16-290055.7 being a bright cataclysmic variable; the observed period of ≈ 215 days is potentially the orbital period of the evolved star around an accreting white dwarf.

5.20. PSD J174541.39-290126.6

PSD J174541.39-290126.6 is one of the reddest stars in our sample, with an observed $H-K = 4.3$. In *H*-band we observe an amplitude of ≈ 1 mag, though the more coherent *K*-band light curve only shows variations of $\Delta m_K \approx 0.6$ mag. Both Wood *et al.* (1998) and Glass *et al.* (2001) find this object (their 61-7 and 3-205 respectively) to have an amplitude of $\approx 0.8-0.9$ mag and a period of ≈ 515 days, both of which are consistent with our data. Furthermore, Wood *et al.* (1998) associate this large-amplitude variable with the OH/IR star OH 359.932-0.059 (Sjouwerman 1997).

5.21. PSD J174542.36-290011.2

PSD J174542.36-290011.2 is a periodic source with $P \approx 220$ days and amplitudes $\Delta m_H = 0.61$ mag and $\Delta m_K = 0.45$ mag. PSD J174542.36-290011.2 shows regular brightness variations over a period of 110.8 days, but when phased at a period of 221.6 days, both the maxima and the minima are less extreme in the first half of the oscillation than in the second. While minima alternating between shallow and deep is characteristic of an RV Tau type star, a period of ≈ 220 days is too long for PSD J174542.36-290011.2 to be an RV Tau type star (Sterken and Jaschek 1996).

5.22. PSD J174543.14-290050.2

We observe PSD J174543.14-290050.2 to have amplitudes of $\Delta H \approx 0.9$ mag and $\Delta K \approx 0.6$ mag. While it does appear to be periodic, the actual period is not clear; it is possible that the period varies from cycle to cycle. Based on these observations, we propose that PSD J174543.14-290050.2 is an LPV.

6. Summary

We present a catalog of variable stars within ≈ 2 pc of Sgr A* in the near-infrared H and K bands over a three-year baseline; $\approx 80\%$ of these variables are previously unidentfied. This is the first photometric variability study of the Galactic center to use the technique of image subtraction.

We find several new periodic sources. Of these, PSD J174535.60-290035.4 and PSD J174538.34-290036.7 have the shortest periods, with $P \approx 42$ days. We believe PSD J174535.60-290035.4 is a pulsating variable, though it is unlikely to be a Cepheid. PSD J174538.34-290036.7 appears to be a nearly edge-on contact eclipsing binary system, in which case the period is actually 84.8 ± 1.6 days and the individual components are likely to be quite large. Another periodic source, PSD J174540.16-290055.7 ($P \approx 215$ days), is coincident with the X-ray variable CXOGC J174540.1-290055; we suspect that this source is a cataclysmic variable. Among the previously identified sources in the catalog, we associate IRS 10* with a bright X-ray point source and OH, H_2O, and SiO masers, suggesting that it is an AGB star with an accreting companion.

Acknowledgements. David Gonzalez and Juan Espinoza collected all the imaging data used in this paper, and we are grateful for their dedication and competence. The CTIO/Yale 1.0 m telescope and ANDICAM are operated by the SMARTS consortium. We would like to thank Vincent Fish for explaining masers and Marc Pinsonneault for explaining stars to us. We also thank Joel Hartman for his useful

FLUX2MAG and VARTOOLS programs, Grzegorz Pojmański for his excellent LC program, John Beacom, Andy Gould, and Rick Pogge for helpful discussions, and the anonymous referee for thoughtful comments.

REFERENCES

Alard, C. 2000, *Astron. Astrophys. Suppl. Ser.*, **144**, 363.
Alard, C., and Lupton, R.H. 1998, *Astrophys. J.*, **503**, 325.
Benedict, G.F., *et al.* 2007, *Astron. J.*, **133**, 1810.
Blackman, E.G., Frank, A., Markiel, J.A., Thomas, J.H., and Van Horn, H.M. 2001, *Nature*, **409**, 485.
Blum, R.D., Ramírez, S.V., Sellgren, K., and Olsen, K. 2003, *Astrophys. J.*, **597**, 323.
Blum, R.D., Sellgren, K., and DePoy, D.L. 1996a, *Astrophys. J.*, **470**, 864.
Blum, R.D., Sellgren, K., and DePoy, D.L. 1996b, *Astron. J.*, **112**, 1988.
Clark, J.S., Larionov, V.M., and Arkharov, A. 2005, *Astron. Astrophys.*, **435**, 239.
Deguchi, S., Fujii, T., Miyoshi, M., and Nakashima, J.-I. 2002, *PASJ*, **54**, 61.
DePoy, D.L., *et al.* 2003, in: "Instrument Design and Performance for Optical/Infrared Ground-based Telescopes", Edited by Iye, Masanori; Moorwood, Alan F.M. *Proceedings of the SPIE*, Volume **4841**, pp. 827-838.
DePoy, D.L., Pepper, J., Pogge, R.W., Stutz, A., Pinsonneault, M., and Sellgren, K. 2004, *Astrophys. J.*, **617**, 1127.
Efstathiou, G. 2000, *MNRAS*, **317**, 697.
Eisenhauer, F., *et al.* 2005, *Astrophys. J.*, **628**, 246.
Genzel, R., Thatte, N., Krabbe, A., Kroker, H., and Tacconi-Garman, L.E. 1996, *Astrophys. J.*, **472**, 153.
Glass, I.S., Matsumoto, S., Carter, B.S., and Sekiguchi, K. 2001, *MNRAS*, **321**, 77.
Hartman, J.D., Bakos, G., Stanek, K.Z., and Noyes, R.W. 2004, *Astron. J.*, **128**, 1761.
Jackson, J.M., Geis, N., Genzel, R., Harris, A.I., Madden, S., Poglitsch, A., Stacey, G.J., and Townes, C.H. 1993, *Astrophys. J.*, **402**, 173.
Karovska, M., Schlegel, E., Hack, W., Raymond, J.C., and Wood, B.E. 2005, *Astrophys. J. Letters*, **623**, L137.
Kastner, J.H., and Soker, N. 2004a, *Astrophys. J.*, **608**, 978.
Kastner, J.H., and Soker, N. 2004b, *Astrophys. J.*, **616**, 1188.
Krabbe, A., Genzel, R., Eckart, A., Najarro, F., Lutz, D., Cameron, M., Kroker, H., Tacconi-Garman, L.E., Thatte, N., Weitzel, L., Drapatz, S., Geballe, T., Sternberg, A., and Kudritzki, R. 1995, *Astrophys. J. Letters*, **447**, L95.
Lacy, J.H., Townes, C.H., and Hollenbach, D.J. 1982, *Astrophys. J.*, **262**, 120.
Laney, C.D., and Stobie, R.S. 1994, *MNRAS*, **266**, 441.
Levine, D.A., Figer, D.F., Morris, M., and McLean, I.S. 1995, *Astrophys. J. Letters*, **447**, L101.
Lindqvist, M., Winnberg, A., and Forster, J.R. 1990, *Astron. Astrophys.*, **229**, 165.
Lindqvist, M., Winnberg, A., Habing, H.J., and Matthews, H.E. 1992,, *Astron. Astrophys. Suppl. Ser.*, **92**, 43.
Martins, F., *et al.* 2006,, *Astrophys. J. Letters*, **649**, L103.
Menten, K.M., Reid, M.J., Eckart, A., and Genzel, R. 1997, *Astrophys. J. Letters*, **475**, L111.
Muno, M.P., *et al.* 2004, *Astrophys. J.*, **613**, 1179.
Najarro, F., Krabbe, A., Genzel, R., Lutz, D., Kudritzki, R.P., and Hillier, D.J. 1997, *Astron. Astrophys.*, **325**, 700.
Nayakshin, S., and Sunyaev, R. 2005, *MNRAS*, **364**, L23.
Ott, T., Eckart, A., and Genzel, R. 1999, *Astrophys. J.*, **523**, 248.
Paumard, T., *et al.* 2006, *Astrophys. J.*, **643**, 1011.
Peeples, M.S., Bonanos, A.Z., DePoy, D.L., Stanek, K.Z., Pepper, J., Pogge, R.W., Pinsonneault, M.H., and Sellgren, K. 2007, *Astrophys. J. Letters*, **652**, L61.

Rafelski, M., Ghez, A.M., Hornstein, S.D., Lu, J.R., and Morris, M. 2007, *Astrophys. J.*, **659**, 1241.
Reid, M.J., and Moran, J.M. 1981, *Ann. Rev. Astron. Astrophys*, **19**, 231.
Samus, N.N., and Durlevich, O.V. 2004, *VizieR Online Data Catalog*, **2250**, 0.
Scannapieco, E., Silk, J., and Bouwens, R. 2005, *Astrophys. J. Letters*, **635**, L13.
Scargle, J.D. 1982, *Astrophys. J.*, **263**, 835.
Schlegel, D.J., Finkbeiner, D.P., and Davis, M. 1998, *Astrophys. J.*, **500**, 525.
Schwarzenberg-Czerny, A. 1996, *Astrophys. J. Letters*, **460**, L107.
Scoville, N.Z., Stolovy, S.R., Rieke, M., Christopher, M., and Yusef-Zadeh, F. 2003, *Astrophys. J.*, **594**, 294.
Silk, J. 1997, *Astrophys. J.*, **481**, 703.
Sjouwerman, L.O. 1997, PhD thesis, AA (Onsala Space Observatory, Sweden).
Sjouwerman, L.O., Lindqvist, M., van Langevelde, H.J., and Diamond, P.J. 2002, *Astron. Astrophys.*, **391**, 967.
Skrutskie, M.F., *et al.* 2006, *Astron. J.*, **131**, 1163.
Soker, N., and Zoabi, E. 2002, *MNRAS*, **329**, 204.
Soszyński, I., Udalski, A., Kubiak, M., Szymański, M.K., Pietrzyński, G., Żebruń, K., Wyrzykowski, Ł., and Dziembowski, W.A. 2004, *Acta Astron.*, **54**, 347.
Sterken, C., and Jaschek, C. 1996, "Light Curves of Variable Stars, A Pictorial Atlas", ISBN 0521390168, Cambridge University Press, 1996..
Stetson, P.B. 1987, *P.A.S.P.*, **99**, 191.
Stetson, P.B. 1992, *Journal Royal Astronomical Society of Canada*, **86**, 71.
Tamura, M., Werner, M.W., Becklin, E.E., and Phinney, E.S. 1996, *Astrophys. J.*, **467**, 645.
Trippe, S., *et al.* 2006, *Astron. Astrophys.*, **448**, 305.
van der Hucht, K.A. 2001, *New Astronomy Review*, **45**, 135.
Wood, P.R., Habing, H.J., and McGregor, P.J. 1998, *Astron. Astrophys.*, **336**, 925.